Supplementary information

Molecular basis of HACD-TECR complex mediated very-long-chain fatty acid elongation reveal a potential target in colorectal cancer

Rui Lv[1,2,#], Leiye Yu[1,3,#], Jingyi Liu[2,4,#], Youli Zhou[5,6,#], Ruiping He[1,#], Chen Wang[1], Bing Gan[1], Rujuan Ti[7], Haizhan Jiao[5], Baohui Song[4], Yiqi Chen[1], Feifei Lin[8], Mei Gao[6], Hongli Hu[5], Shankai Yin[3], Pinghong Zhou[4], Lizhe Zhu[7], Mingyan Cai[4], Tian Xie[9,*], Jia Liu[8,*], Li Chen[1,10,*], Yunshi Zhong[2,4,*], Ruobing Ren[1,2,*]

[1] Shanghai Key Laboratory of Metabolic Remodeling and Health, Institute of Metabolism and Integrative Biology, Fudan University, Shanghai 200437, China

[2] Shanghai Xuhui Central Hospital, Zhongshan-Xuhui Hospital, Fudan University, Shanghai 200020, China

[3] Department of Otorhinolaryngology Head and Neck Surgery, Shanghai Sixth People's Hospital Affiliated to Shanghai Jiao Tong University School of Medicine, Shanghai 200233, China

[4] Endoscopy Center and Endoscopy Research Institute, Zhongshan Hospital, Fudan University, Shanghai 200032, China

[5] Kobilka Institute of Innovative Drug Discovery, School of Medicine, The Chinese University of Hong Kong, Shenzhen, Guangdong 518172, China

[6] Central Research Laboratories, Chongqing General Hospital, Chongqing University & Chongqing Academy of Medical Sciences, 118 Xingguang Avenue, Liangjiang New Area, Chongqing 401147, China

[7] Warshel Institute of Computational Biology, School of Medicine, The Chinese University of Hong Kong, Shenzhen, Guangdong 518172, China

[8] China-Serbia "Belt and Road" Joint Laboratory for Natural Products and Drug Discovery, Shanghai Institute of Materia Medica, Chinese Academy of Sciences, 555 Zuchongzhi Road, Zhangjiang Hitech Park, Shanghai 201203, China

[9] MOE Key Laboratory of Geriatric Diseases and Immunology, Biomedical Basic Research Center of Jiangsu, Institute of Molecular Enzymology, School of Life Sciences, Suzhou Medical College of Soochow University, Suzhou,

Jiangsu, 215123, China

[10] Obstetrics and Gynecology Hospital, Fudan University, Shanghai 200438, China

[#] These authors contributed equally

[*] To whom correspondence should be addressed. Email: renruobing@fudan.edu.cn

Supplementary methods

Bioinformatics

For TECR expression analysis between human cancers and normal tissues, we conducted bioinformatics analysis on UCSC Xena (https://xenabrowser.net/). It is an online analysis tool for processing high-throughput RNA sequencing expression data of bulk tumorous and normal samples based on the Cancer Genome Atlas (TCGA) (https://portal.gdc.cancer.gov/), the Genotype-Tissue Expression (GTEx, https://www.gtexportal.org/) and Gene Expression Omnibus (GEO) (accession number GSE184093) databases. Log2-transformed FPKM values were used as normalized gene expression levels. Group differences were compared using the ggpubr R package, and statistical significance was assessed with Student's independent t-test. Graphs were constructed using GraphPad Prism (10.0, La Jolla, CA, USA) and R software.

The scRNA-seq dataset of colorectal cancer was retrieved from the Gene Expression Omnibus (GEO) database under accession number GSE132465. Data processing and downstream analyses were performed using the Seurat R package (version 5). To ensure consistency with the source studies, cell type annotations were adopted directly from the original metadata provided by the respective authors. The global cellular landscape was visualized using Uniform Manifold Approximation and Projection (UMAP) for dimensionality reduction. Furthermore, to investigate the role of TECR in tumor progression, its expression levels within the malignant epithelial cell subpopulation were specifically evaluated. Differential expression analysis was performed using the Wilcoxon rank-sum test, with statistical significance determined by adjusted P-values.

Cell lines and culture protocols

The HCT116, SW480, and SW620 cell lines were purchased from the Culture Collection of the Chinese Academy of Sciences, Shanghai, China (http://www.cellbank.org.cn/). The HEK293T cell line was obtained from the American Type Culture Collection (ATCC). The OVSAHO, and A2780S cell lines were kindly provided by Shengtao Zhou (Sichuan University). The ISHIKAWA cell line was a kind gift from Lingbo Wang. The LICCF, REB, and TFK-1 cell lines were gifts from Hongyang Wang (Fudan University). The MDA-MB-231, HuH7, and HeLa cell lines were gifts from Tongjin Zhao (Fudan University). The LICCF, REB, TFK-1 cells were cultured in RPMI-1640 medium (Macgene, CM10041) supplemented with 10% (v/v) fetal bovine serum (Every green, 11011-8611). The other cell lines were cultured in DMEM medium (Macgene, CM10013) supplemented with 10% Fetal Bovine Serum (FBS) at 37°C in an atmosphere of 5% CO_2.

Generation of knockdown or knockout cell lines

For the transient knockdown (KD) of TECR, the anti-TECR siRNA (siTECR1 or siTECR2) was directly transfected into the various cancer cell lines for cell proliferation assays. All transfections were performed using Lipofectamine™ 3000 Reagent (Invitrogen, L3000015) according to the manufacturer's instructions.

For the stable knockdown of TECR, the anti-TECR shRNA (shTECR1 or shTECR2) was inserted into the pLKO.1 plasmid and co-transfected with viral packaging plasmids (psPAX2 and pMD2.G) using PEI 4000 (Polysciences, 24885-2) into HEK293T cells to generate and amplify lentivirus first. After transfection for 48 hours, the virus was collected from the culture medium and filtered through a 0.45 μm filter. The HCT116 and SW480 cell lines were infected with the virus for 48 hours and then selected with 2 μg/mL puromycin for one week to generate the stable TECR-KD cell lines for further experiments.

For the stable knockout (KO) of TECR using the CRISPR-Cas9 system, the anti-TECR single-guide RNA (sgRNA) was cloned into the lentiCRISPR v2 plasmid and co-transfected with the same viral packaging plasmids into HEK293T cells to generate lentivirus similarly. The lentivirus was collected from the media after transfection for 48 hours. The HCT116 cells were infected with the lentivirus for 48 hours and selected with 2 μg/mL puromycin for 4-5 weeks to generate monoclonal stable TECR-KO cell lines for further experiments.

Cell proliferation assay

Cell proliferation was evaluated using the Cell Counting Kit-8 (Yeasen Biotech, 40203ES80) based on the manual. Briefly, about 1 × 10^3 cells were seeded in the 96-well plates with three replicates for each group. After cell attachment, the CCK-8 reagent was added at the indicated time points (1 day, 2 days, 3 days, 4 days, and 5 days). Following incubation at 37°C for 1 hour, the absorbance at 450 nm was measured using a microplate reader to determine cell viability.

Colony formation assays and crystal violet staining

About 1~2 × 10^3 HCT116 or SW480 cells (control or TECR-KD cells) were seeded in the 6-well cell culture plates with the complete cell culture medium (DMEM with 10% FBS) and cultured for 10~14 days. Then the cells were fixed with 4% paraformaldehyde in PBS for 10 minutes at room temperature and stained with 0.1% crystal violet staining (Servicebio; G1014) to assess the colony formation capacity of the cells.

Invasion and migration assay

Cell migration and invasion assays were conducted using transwell chambers with 8-μm pore membranes (BIOFIL; TCS020024). For the migration assay, 1 × 10^5 HCT116 or SW480 cells (control or

TECR-KD cells) were suspended in 200 μL of serum-free DMEM medium and seeded into the upper chamber, while the lower chamber was filled with 700 μL of DMEM medium containing 10% FBS as a chemoattractant. After incubation for 24~48 hours at 37°C, non-migrated cells remaining on the upper surface were gently removed with a cotton swab. The migrated cells on the lower surface of the membrane were fixed with 4% paraformaldehyde for 10 minutes, stained with 0.1% crystal violet for 10 minutes, and imaged under a light microscope. For the invasion assay, the upper chambers were pre-coated with 50 μL of Matrigel (Absin, abs9490; diluted 1:8 in serum-free DMEM) and incubated at 37°C for 1 hour before cell seeding. The subsequent steps were performed in the same manner as for the migration assay.

Cell cycle assay

The HCT116 cells (control or TECR-KD cells) grown in the logarithmic phase were stained using a PI Staining Kit (Solarbio; C0080). Briefly, the cells were incubated with a 20 μg/mL staining solution for 20 minutes at 37°C. After washing with PBS, cells were analyzed via flow cytometry within 30 minutes. All procedures were performed in the dark.

Animal studies

Male BALB/c nude mice (6 weeks old) were used for the subcutaneous xenograft tumor model. Briefly, 1×10^6 HCT116 cells (control or TECR-KD cells) suspended in 0.2 mL of PBS were subcutaneously injected into the flank of each mouse. Tumor growth was monitored every 2 days, and tumor volume was calculated using the formula: volume = (length $\times$ width^2) / 2. Mice were euthanized 14 days after cell injection, and the tumors were excised, photographed, and weighed for subsequent analysis. All animal experiments were approved by the Institutional Animal Care and Use Committee and performed

by institutional guidelines.

Sample collections

This study included 261 tissue samples in the colorectal tumor tissue microarray, comprising 87 matched pairs of normal intestinal mucosa, colorectal adenoma, and colorectal cancer tissues from 87 patients with colorectal cancer. All samples were collected from Zhongshan Hospital, Fudan University, Shanghai, between September 2020 and September 2022. All enrolled patients met the inclusion criteria of receiving no comprehensive treatment, including radiotherapy or chemotherapy, before sampling. The Ethics Committee of Zhongshan Hospital, Fudan University approved the study protocol. The pathological diagnosis of all tissue specimens was independently confirmed by two experienced pathologists.

Immunochemistry (IHC)

Immunohistochemical staining was performed on paraffin-embedded tissue microarrays (TMAs) derived from human colorectal cancer (CRC) specimens. The staining procedure was conducted using a commercial immunohistochemical detection kit (Zhongshan Jinqiao Biotechnology; SP-9000) following the manufacturer's protocol. The primary antibodies used in the experiments included anti-TECR primary antibody (1:200 dilution; Abcam; ab247124). For the TMAs, TECR expression levels were semi-quantitatively evaluated using the H-score method. The H-score was calculated using the formula: H-score = $\sum$(Pi×i) = (percentage of weakly stained cells×1) + (percentage of moderately stained cells × 2) + (percentage of strongly stained cells × 3)[1-3].

Immunofluorescent staining

The xenograft tumor tissues from nude mice were fixed in 4% paraformaldehyde for 24 hours at room

temperature, paraffin-embedded, and serially sectioned at 5 μm. Sections were treated with 3% H_2O_2 and subjected to heat-induced antigen retrieval in citrate buffer (pH 6.0). Upon cooling to room temperature, nonspecific binding was blocked with 3% BSA. Sections were then incubated overnight at 4°C with the primary antibody (1:500; Servicebio; GB111499). Following PBS washes, samples were stained with a fluorophore-conjugated secondary antibody (1:300; Servicebio; GB25303) and mounted with DAPI-containing medium.

LC/MS analysis of fatty acids in cell extracts

To analyze the total cellular fatty acids, a total of 4 × 10^6 HCT116 cells (control or TECR-KO cells) were resuspended with 0.9 mL of an ice-cold methanol:isopropanol (MeOH:IPA, 1:1, v/v) mixture. The lipids were saponified by adding 0.1 mL 3 M KOH and heated at 60°C for 1 h, and the mixture was acidified by adding 0.1 mL formic acid after cooling down. The saponified fatty acids were extracted with hexane, dried down by N2 flow, and resuspended in methanol:isopropanol (MeOH:IPA, 1:1, v/v) mixture. Lipid extracts were analyzed using a Vanquish F UHPLC system (Thermo Fisher Scientific) coupled with a Thermo Orbitrap Exploris 480 mass spectrometer. Chromatographic separation was achieved on an Acclaim C30 column (3 μm, 2.1 × 150 mm) maintained at 45°C. The mobile phase consisted of solvent A (10 mM ammonium formate with 0.1% formic acid in water:acetonitrile 40:60, v/v) and solvent B (10 mM ammonium formate with 0.1% formic acid in isopropanol:acetonitrile 90:10, v/v). The flow rate was set to 0.26 mL/minute with a gradient elution program as follows: 0-2 minutes, 15% B; 3 minutes, 30% B; 10.5 minutes, 45% B; 14 minutes, 97% B; 14-18 minutes, hold at 97% B; 18-18.1 minutes, return to 15% B; and 18.1-25 minutes, re-equilibration at 15% B. The injection volume was 10 μL, and the autosampler was maintained at 6°C. Mass spectrometric analysis was performed in negative ion mode using full scan with a scan range of m/z 200–1500. The resolution was set to 240,000 at m/z 200.

Co-IP experiment and peptide-competition assay

For the co-immunoprecipitation (co-IP) experiment with His-tagged human HACD2 and Flag-tagged human TECR, the protein were co-expressed in Expi293 similarly as above. The cells were collected and resuspended in buffer C (25 mM HEPES pH 7.5, 150 mM NaCl, 2% glycerol). The cell lysis was extracted by 1% n-Dodecyl-β-D-Maltopyranoside (DDM; Anatrace) and 0.1% CHS in the presence of protease inhibitors. After centrifugation, the supernatant was immunoprecipitated with Ni-NTA affinity resin. The resin was thoroughly washed with buffer C containing 25mM imidazole and 0.02% DDM and 0.002% CHS. Bound proteins were subsequently eluted using buffer C supplemented with 0.02% DDM, 0.002% CHS, and 250mM imidazole. The eluted samples were analyzed by Western blotting. For the co-immunoprecipitation (co-IP) experiment with C-terminal His-tagged C. elegans HACD and Flag-tagged C. elegans TECR, the codon-optimized HACD and TECR sequences were individually inserted into pMLink vector. The protein co-expression and co-IP experiments were performed similarly as above.

For the peptide-competition assay, the His-tagged human HACD2 and Flag-tagged human TECR were co-expressed in Expi293. After membrane extraction by 1% DDM and 0.1% CHS, the supernatant was incubated with anti-Flag G1 affinity resin. Following washing, the resin was incubated with various peptides at a concentration of 400μg/ml for 1 hour. Then the resin was washed and eluted with the 200 μg/mL Flag peptide for western blotting analysis.

Molecular dynamics simulation

The 3-hydroxyacyl-CoA substrate was docked into the protein by DSDP blind docking module[4]. The Membrane Builder module in CHARMM-GUI server[5] was used to prepare the molecular dynamics (MD) simulation inputs, including a membrane of pre-equilibrated (310 K) POPC lipids based on the

OPM database[6] alignment, TIP3P solvent with 0.15 M Na^+/Cl^- ions and the CHARMM36 force field[7]. The force field of the ligand was generated by the CGenFF program[8]. Three independent 100-ns MD simulations were performed. All MD simulations were performed using GROMACS-2019.4[9]. The CHARMM36 force-field was used to describe the interactions in the system. Energy minimization was performed for 10000 steps by the steepest descent algorithm. Then a 100 ps NVT simulation was performed at 310 K for solvent equilibration, followed by a 1 ns NPT equilibration to 1 atm using the Berendsen barostat[10]. The production simulations were performed with a time-step of 2 fs using Parrinello-Rahman barostat[11]. In all constant temperature simulations, the Bussi (velocity-rescaling) thermostat was used[12]. Long-range electrostatic interactions were treated by the particle-mesh Ewald method[13]. The short-range electrostatic and van der Waals interactions both used a cutoff of 10 Å. All H-bonds were constrained by the LINCS algorithm[14].

References

1. Maclean, A., et al., *Fallopian tube epithelial cells express androgen receptor and have a distinct hormonal responsiveness when compared with endometrial epithelium.* Hum Reprod, 2020. **35**(9): p. 2097-2106.
2. Dogan, S., et al., *DNA methylation-based classification of sinonasal undifferentiated carcinoma.* Mod Pathol, 2019. **32**(10): p. 1447-1459.
3. Paschalis, A., et al., *Prostate-specific Membrane Antigen Heterogeneity and DNA Repair Defects in Prostate Cancer.* Eur Urol, 2019. **76**(4): p. 469-478.
4. Huang, Y., et al., *DSDP: A Blind Docking Strategy Accelerated by GPUs.* J Chem Inf Model, 2023. **63**(14): p. 4355-4363.
5. Jo, S., et al., *CHARMM-GUI: a web-based graphical user interface for CHARMM.* J Comput Chem, 2008. **29**(11): p. 1859-65.
6. Lomize, M.A., et al., *OPM database and PPM web server: resources for positioning of proteins in membranes.* Nucleic Acids Res, 2012. **40**(Database issue): p. D370-6.
7. Huang, J. and A.D. MacKerell, Jr., *CHARMM36 all-atom additive protein force field: validation based on comparison to NMR data.* J Comput Chem, 2013. **34**(25): p. 2135-45.
8. Vanommeslaeghe, K., et al., *CHARMM general force field: A force field for drug-like*

molecules compatible with the CHARMM all-atom additive biological force fields. J Comput Chem, 2010. **31**(4): p. 671-90.
9. Abraham, M.J., et al., *GROMACS: High performance molecular simulations through multi-level parallelism from laptops to supercomputers.* SoftwareX, 2015. **1-2**: p. 19-25.
10. Berendsen, H.J.C., et al., *Molecular dynamics with coupling to an external bath.* The Journal of Chemical Physics, 1984. **81**(8): p. 3684-3690.
11. Parrinello, M. and A. Rahman, *Crystal Structure and Pair Potentials: A Molecular-Dynamics Study.* Physical Review Letters, 1980. **45**(14): p. 1196-1199.
12. Bussi, G., D. Donadio, and M. Parrinello, *Canonical sampling through velocity rescaling.* J Chem Phys, 2007. **126**(1): p. 014101.
13. Darden, T., D. York, and L. Pedersen, *Particle mesh Ewald: An N·log(N) method for Ewald sums in large systems.* The Journal of Chemical Physics, 1993. **98**(12): p. 10089-10092.
14. Hess, B., et al., *LINCS: A linear constraint solver for molecular simulations.* Journal of Computational Chemistry, 1997. **18**(12): p. 1463-1472.

Supplementary figures

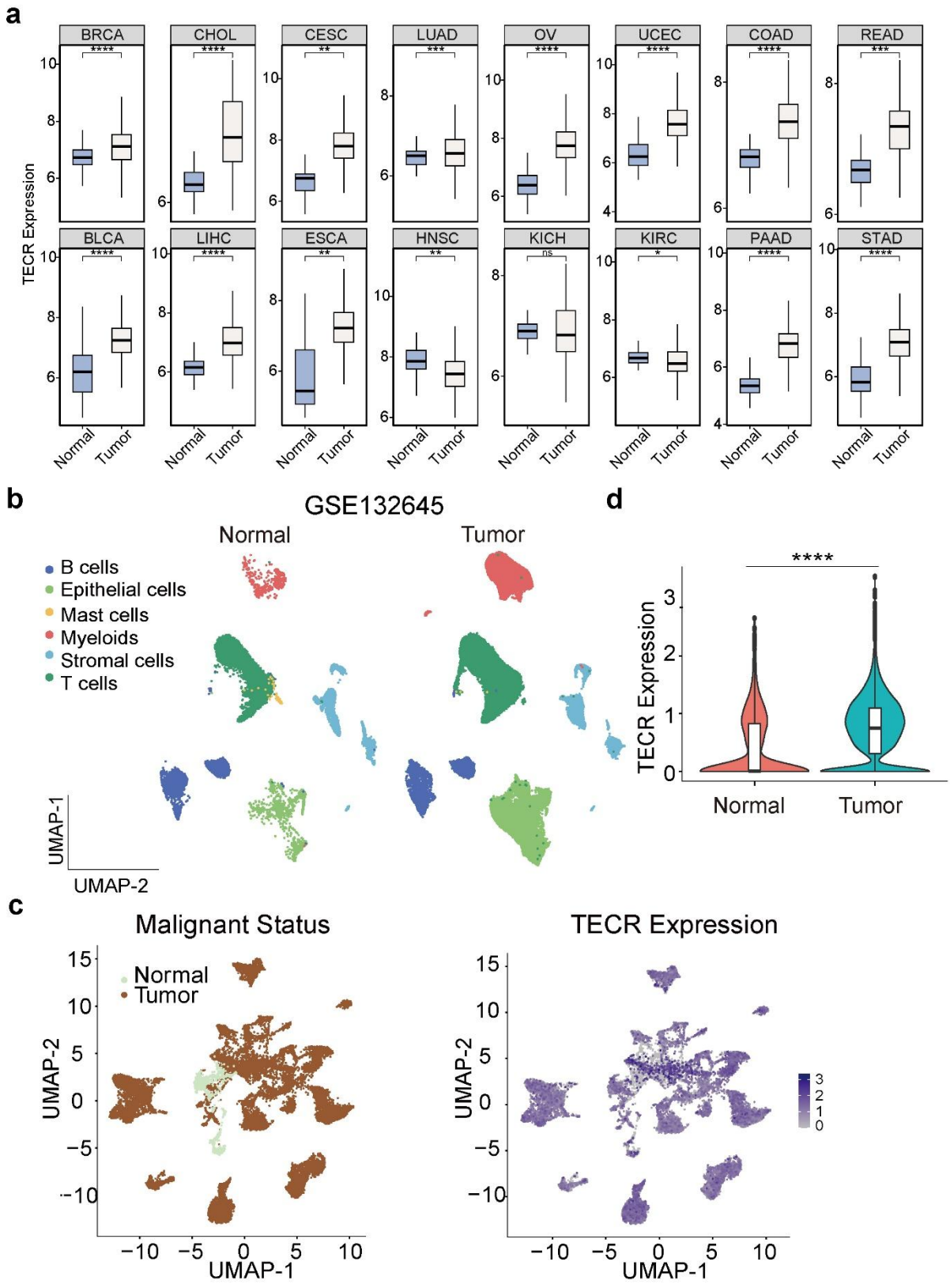

Fig. S1 | TECR is associated with CRC cell proliferation and tumorigenesis. a, Box plots showing

TECR transcription profiles in tumor samples and paired normal tissues. The position of each dot represents the amount of gene transcription level in the sample. **b-d,** UMAP representations of CRC single-cell sequencing dataset from GSE132465. TECR expression in CRC single-cell sequencing data between non-malignant cells and malignant cells from GSE132465. FPKM values were log2-transformed to normalize gene expression data. Significance was determined via an unpaired Student's t-test (a). Differential expression analysis was performed using the Wilcoxon rank-sum test, with statistical significance determined by adjusted P-values (d). *P < 0.05, **P < 0.01, ***P < 0.001, ****P < 0.0001.

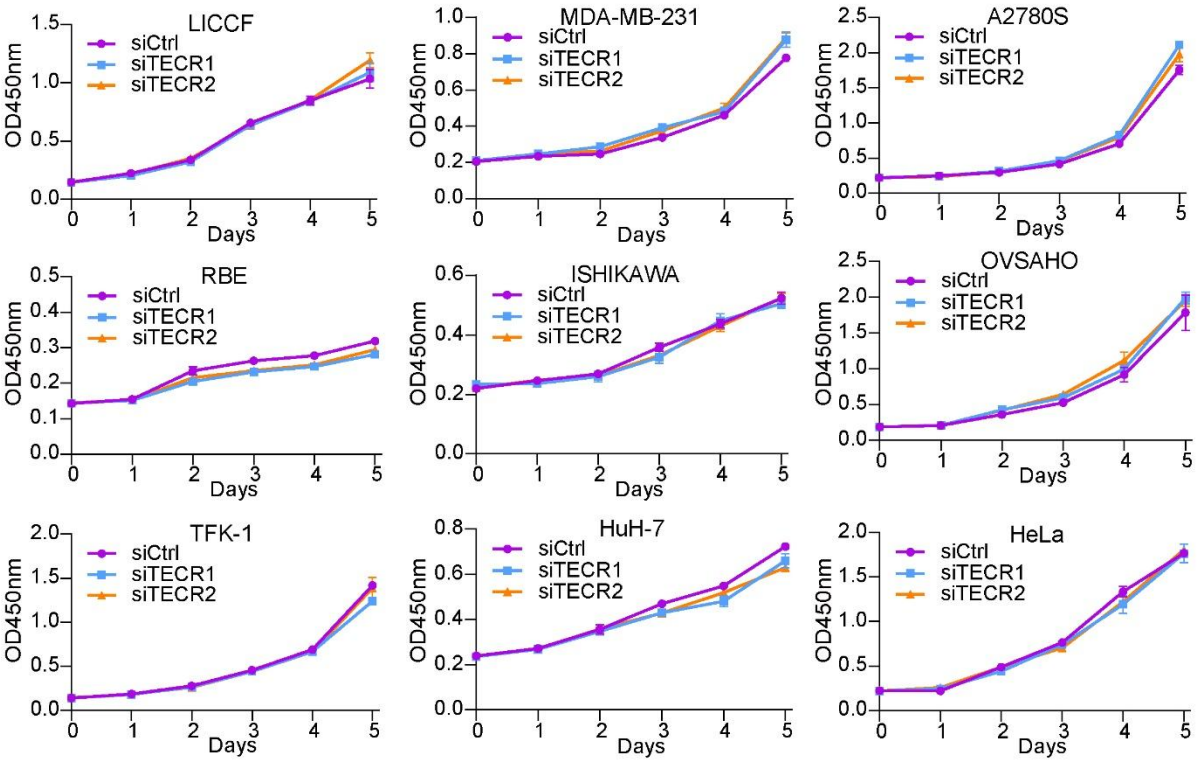

Fig. S2 | Cell proliferation analysis of various cancer cell lines upon TECR knockdown.

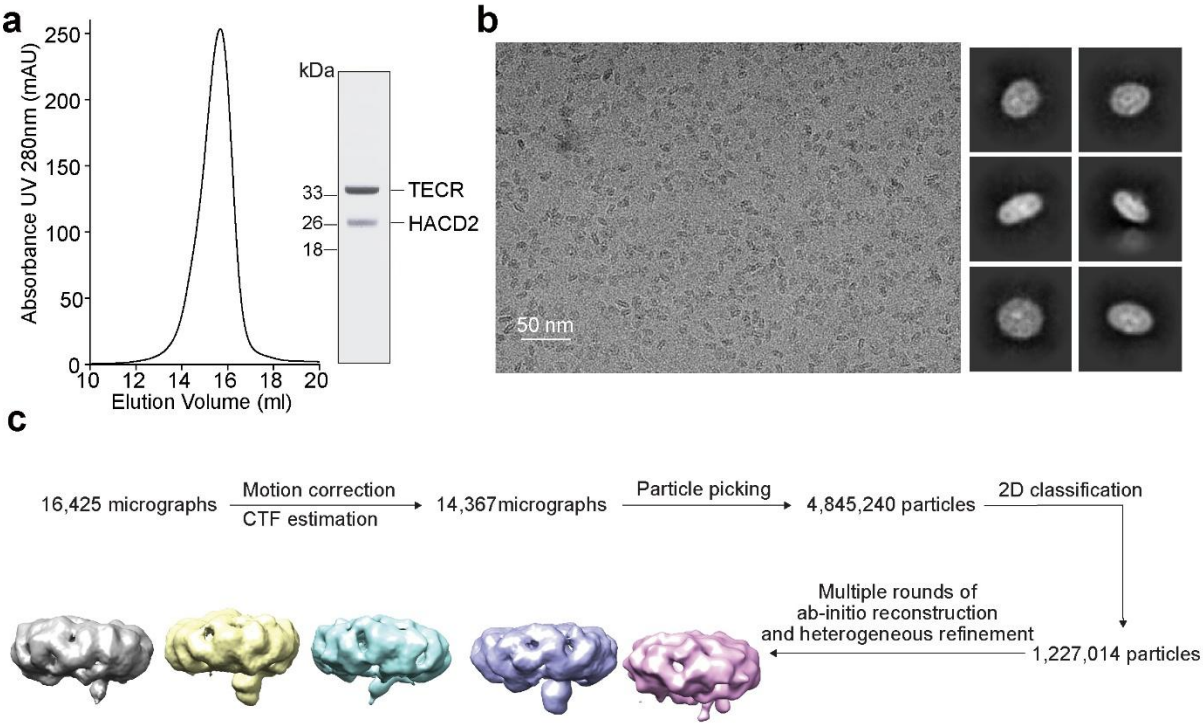

Fig. S3 | **Cryo-EM analysis of the human HACD2-TECR complex. a,** Size-exclusion chromatography (SEC) profile and Coomassie blue-stained SDS-PAGE gel of the purified human HACD2-TECR complex. b**,** Representative cryo-EM image and 2D class averages of the HACD2-TECR complex. **c,** Cryo-EM data processing flowchart of the HACD2-TECR complex datasets.

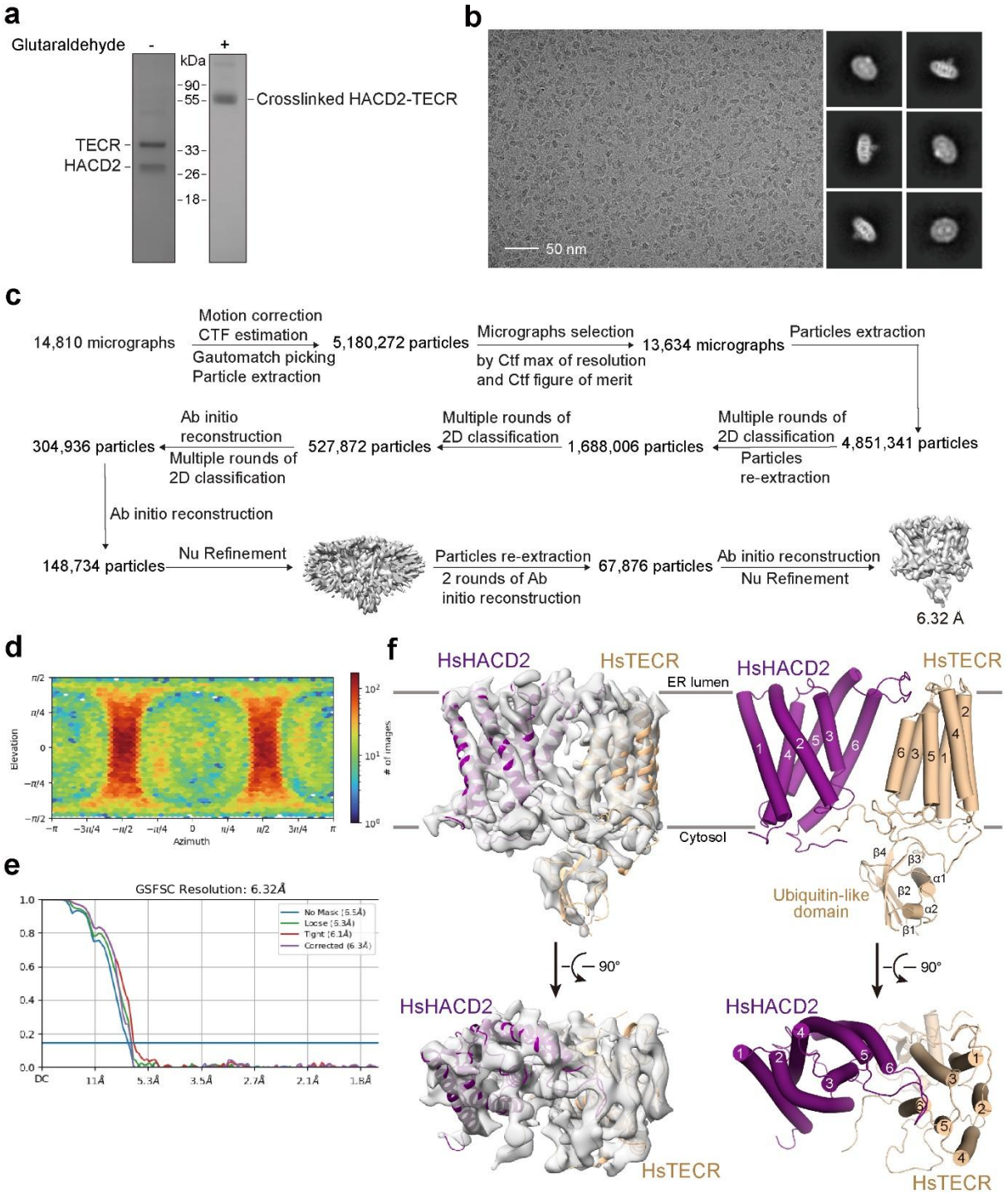

Fig. S4 | Cryo-EM analysis of the crosslinked human HACD2-TECR complex. a, SEC profile and Coomassie blue-stained SDS-PAGE gel of the crosslinked human HACD2-TECR complex. **b,** Representative cryo-EM image and 2D class averages of the crosslinked HACD2-TECR complex. **c,** Cryo-EM data processing flowchart of the crosslinked HACD2-TECR complex dataset. **d-e,** Euler

angle distribution (**d**) and gold-standard FSC curves (**e**) of the crosslinked HACD2-TECR complex. **f,** Cryo-EM map and structural model of the human HACD2-TECR complex. The structural models of HACD2 and TECR predicted by AlphaFold were docked into the moderate-resolution 3D EM map. HACD2 and TECR are colored purple and wheat, respectively.

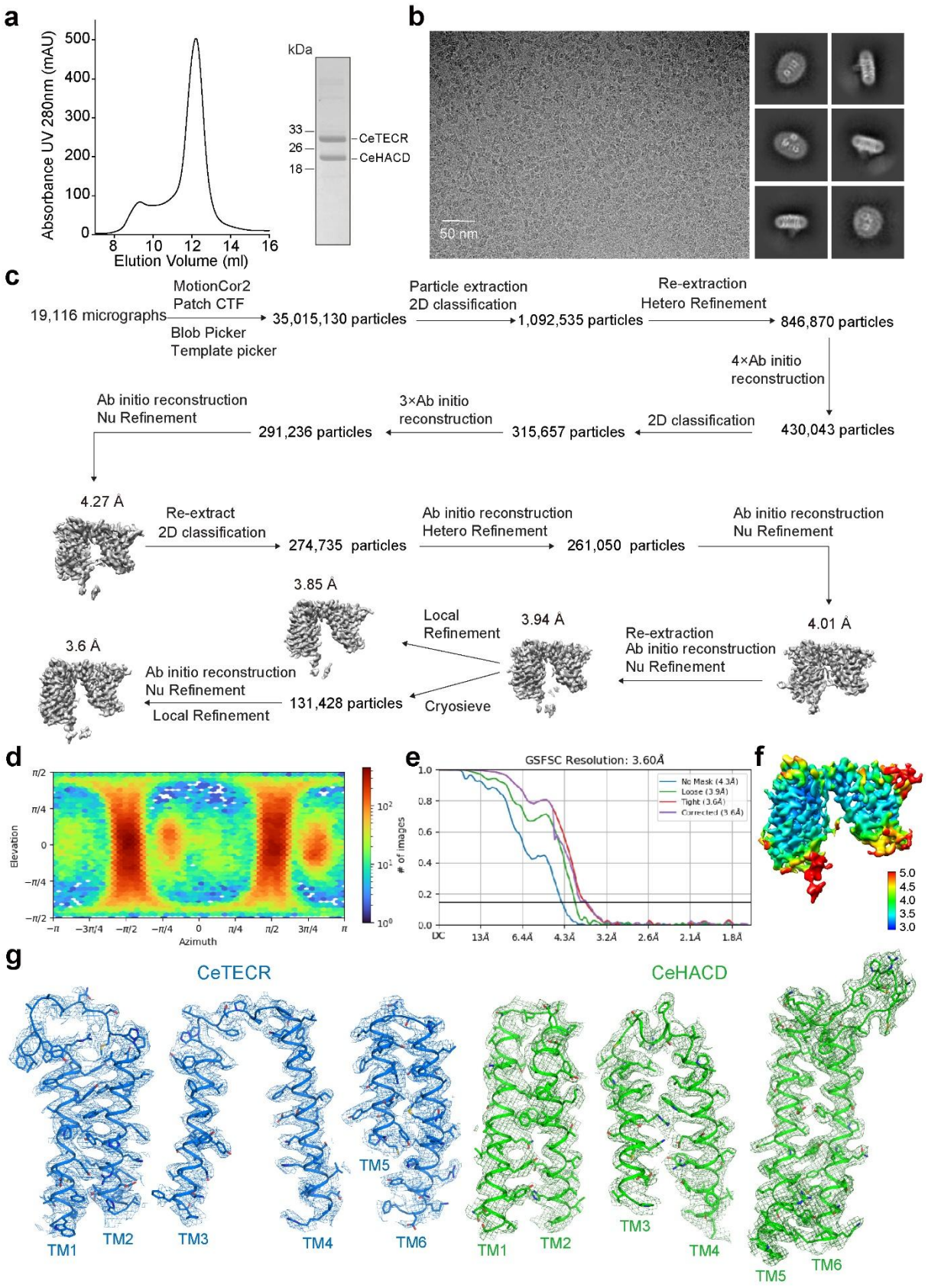

Fig. S5 | Cryo-EM analysis of the *C. elegans* HACD-TECR complex. a, SEC profile and Coomassie blue-stained SDS-PAGE gel of the *C. elegans* HACD-TECR complex. **b,** Representative cryo-EM

image and 2D class averages of the *C. elegans* HACD-TECR complex. **c,** Cryo-EM data processing flowchart of the *C. elegans* HACD-TECR complex. **d-f,** Euler angle distribution (**d**), gold-standard FSC curves (**e**), and local resolution map (**f**) of the *C. elegans* HACD-TECR complex. **g,** Representative density maps of the HACD and TECR subunits, contoured at 5σ.

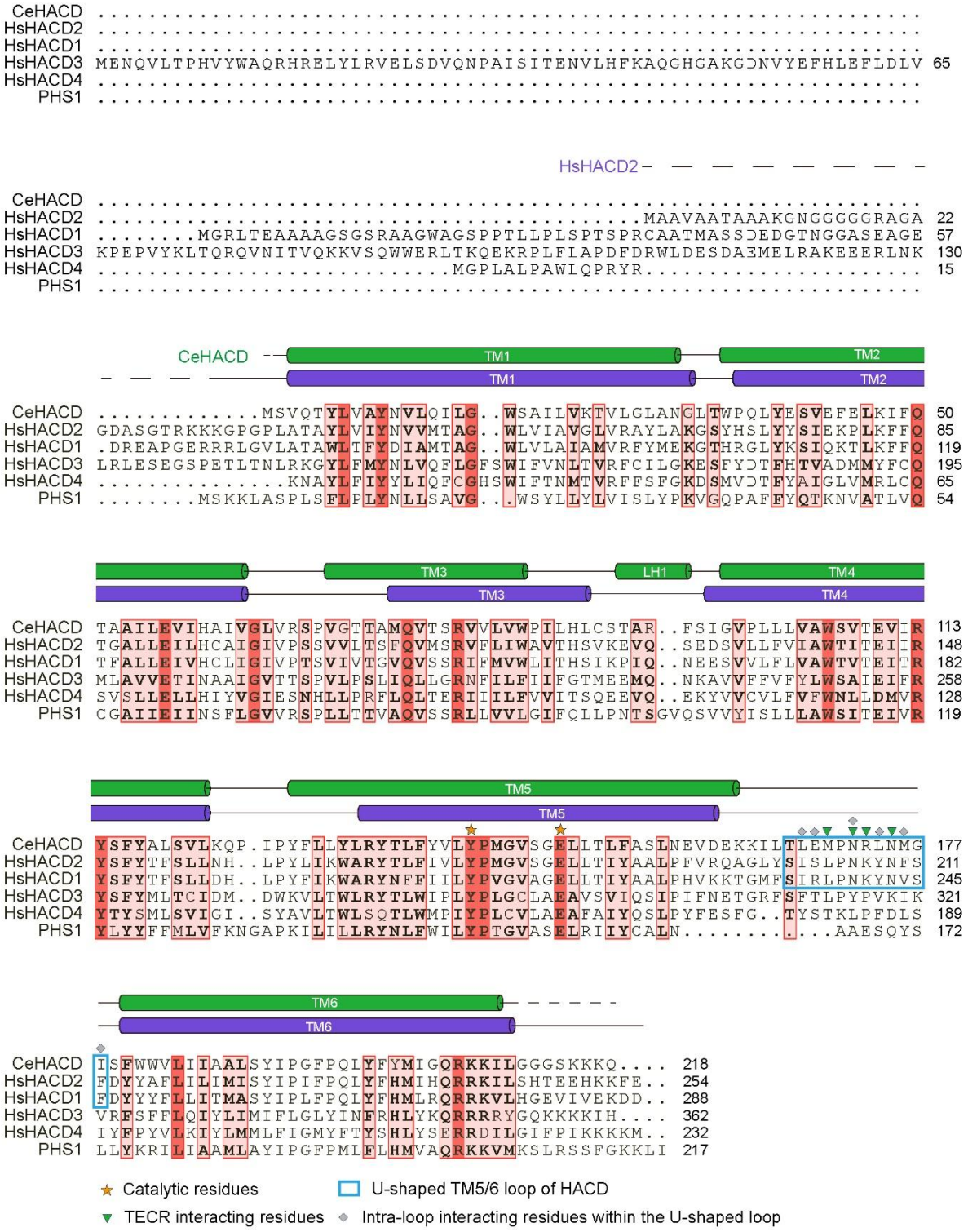

Fig. S6 | **Sequence alignment of HACD homologs.** Secondary structural elements of *C. elegans* HACD and human HACD2 are indicated above the sequence alignment. TM: transmembrane helix; LH: luminal helix. The catalytic residues are indicated by orange stars, while the TECR-binding residues are indicated by green triangles. The U-shaped TM5/6 loop of HACD crucial for TECR

binding is indicated by blue box. The intra-loop interacting residues within the U-shaped loop are indicated by gray diamonds. The UniProt IDs of the aligned sequences are as follows: CeHACD: O17040; HsHACD1: B0YJ81; HsHACD2: Q6Y1H2; HsHACD3: Q9P035; HsHACD4: Q5VWC8; PHS1: P40857. “Ce” for *C. elegans*; “Hs” for Homo sapiens.

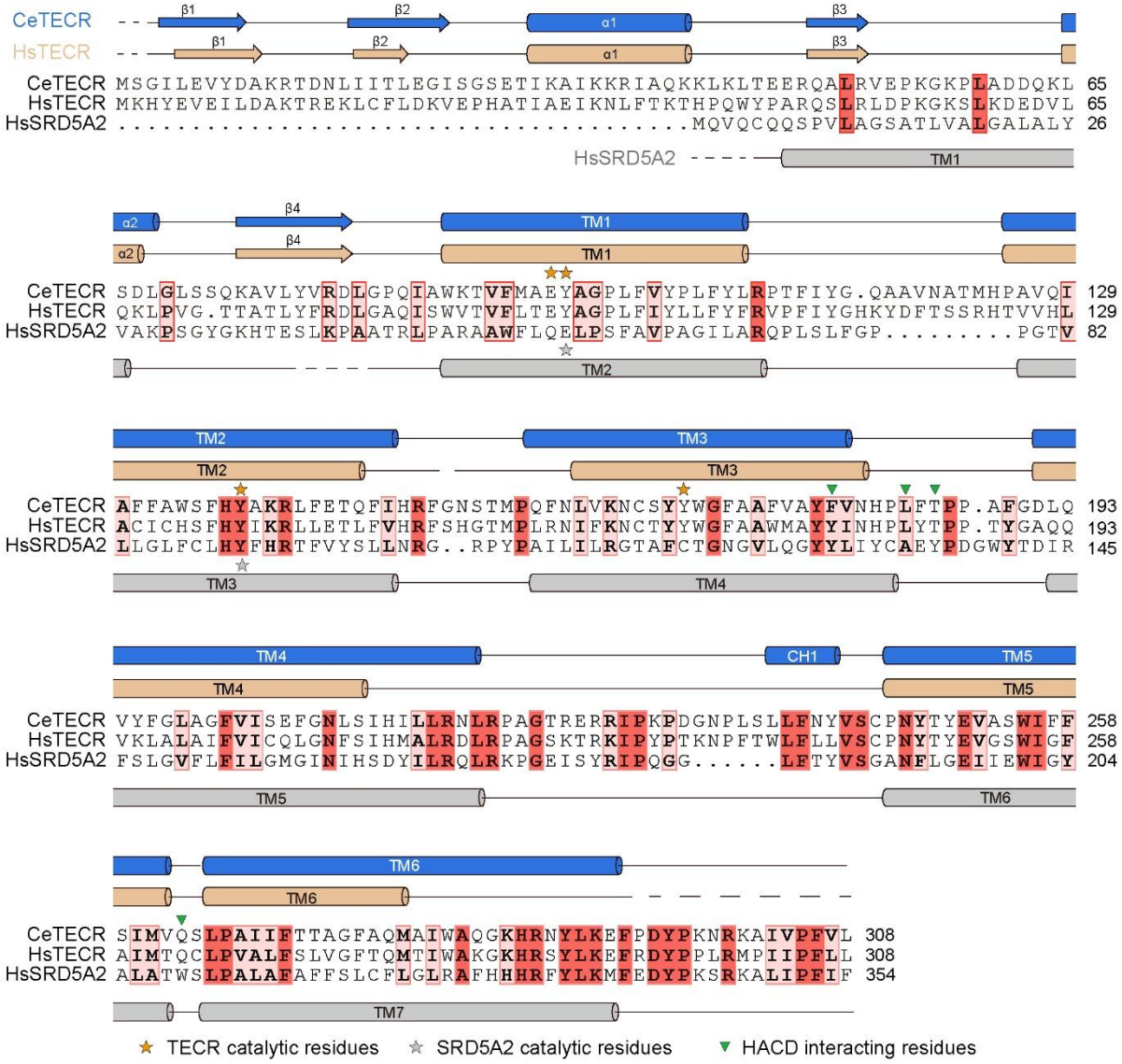

Fig. S7 | Sequence alignment of TECR homologs. Secondary structural elements of *C. elegans* TECR and human TECR are indicated above the sequence alignment. Secondary structural elements of human SRD5A2 are indicated below the sequence alignment. CH: cytosolic helix. The catalytic residues of TECR and SRD5A2 are indicated by orange and gray stars, respectively. The HACD-binding residues on TECR are indicated by green triangles. The UniProt IDs of the aligned sequences are as follows: CeTECR: Q9N5Y2; HsTECR: Q9NZ01; HsSRD5A2: P31213.

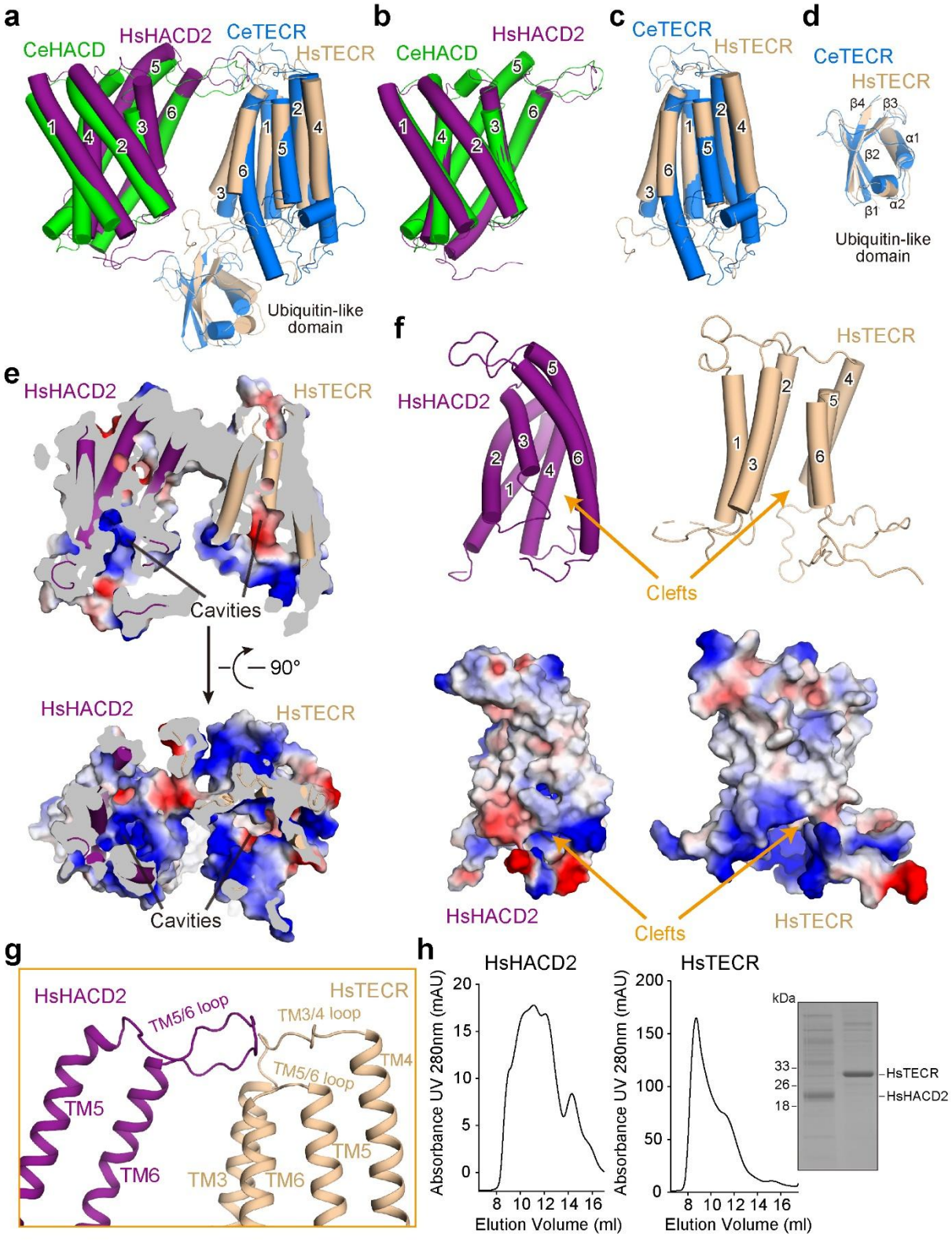

Fig. S8 | Structural comparisons between human HACD2-TECR complex and *C. elegans* HACD-TECR complex. a, Superimposition of human HACD2-TECR complex and *C. elegans* HACD-TECR complex. **b-d,** Superimpositions of the HACD subunits (**b**), TECR transmembrane domains (**c**), and

TECR ubiquitin-like domains (**d**). **e,** Perpendicular views of the central cavities within human HACD2 and TECR transmembrane domains facing the cytosolic side of membrane. **f,** Similar lateral clefts formed by human HACD2-TM3/6 and TECR-TM3/6. **g,** The human HACD2 TM5/6 luminal loop is in close contacts with the TM3/4 and TM5/6 luminal loops of TECR. **h,** SEC profile and Coomassie blue-stained SDS-PAGE gel of purified human HACD2 alone and TECR alone.

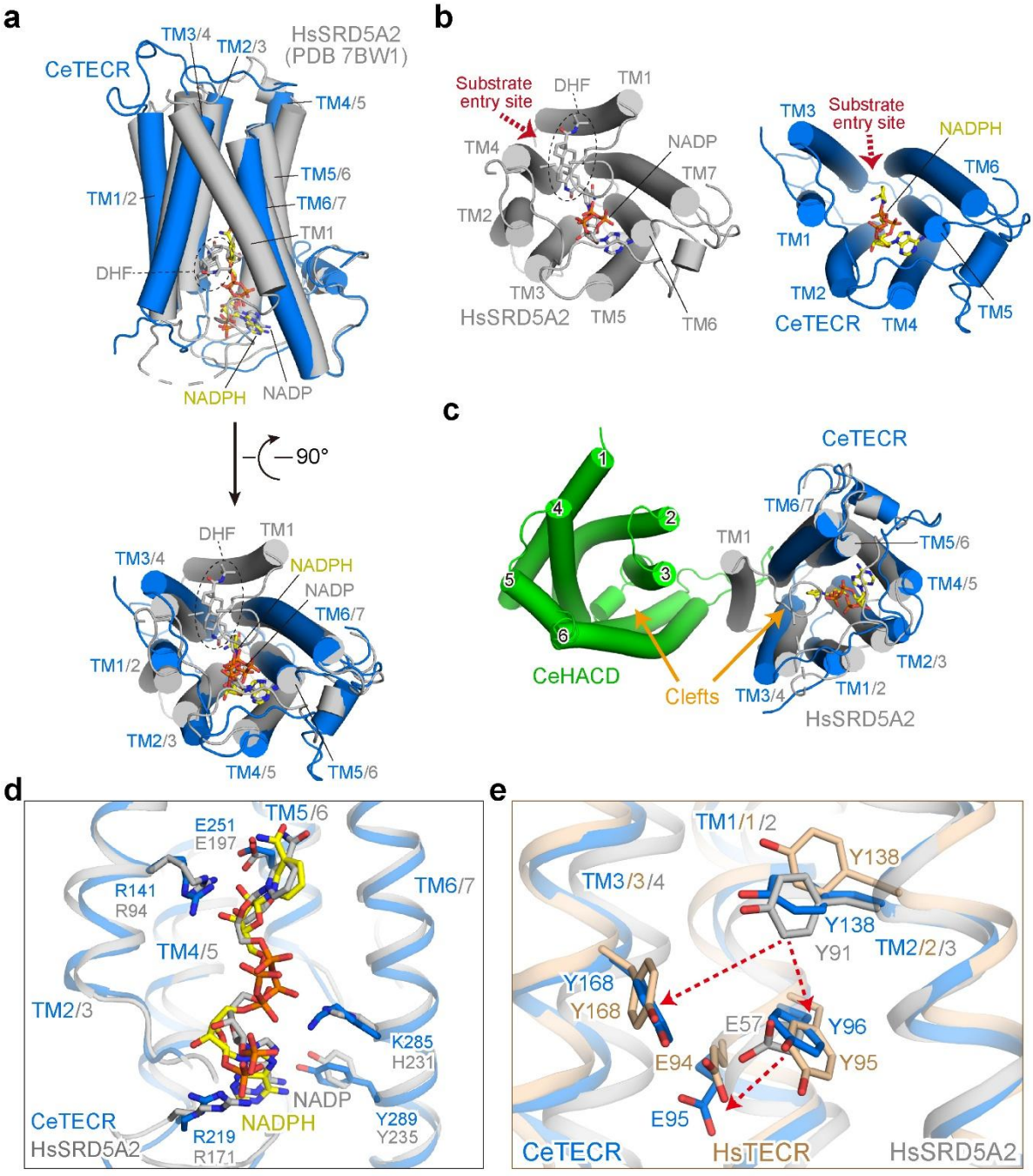

Fig. S9 | **Structural comparisons between TECR and SRD5A2. a,** Superimposition of *C. elegans* TECR subunit with human SRD5A2. The NADP-dihydrofinasteride (NADP-DHF) bound SRD5A2 (PDB 7BW1) and NADPH-bound TECR are colored light grey and blue, respectively. **b,** Potential substrate entry sites on SRD5A2 and TECR. Both SRD5A2 and TECR are presented in the same view with the NADP(H) cofactors located in similar positions. The DHF moiety occupies the potential steroid substrate binding site on SRD5A2. **c,** Superimposition of SRD5A2 and HACD-bound TECR. The TM1

of SRD5A2 is situated between the opposing lateral clefts formed by the TM3/6s of HACD and TECR. **d,** Superimposition of the NADPH coordination residues in *C. elegans* TECR and SRD5A2. **e,** Superimposition of the catalytic residues of *C. elegans* TECR subunit, human TECR subunit, and SRD5A2.

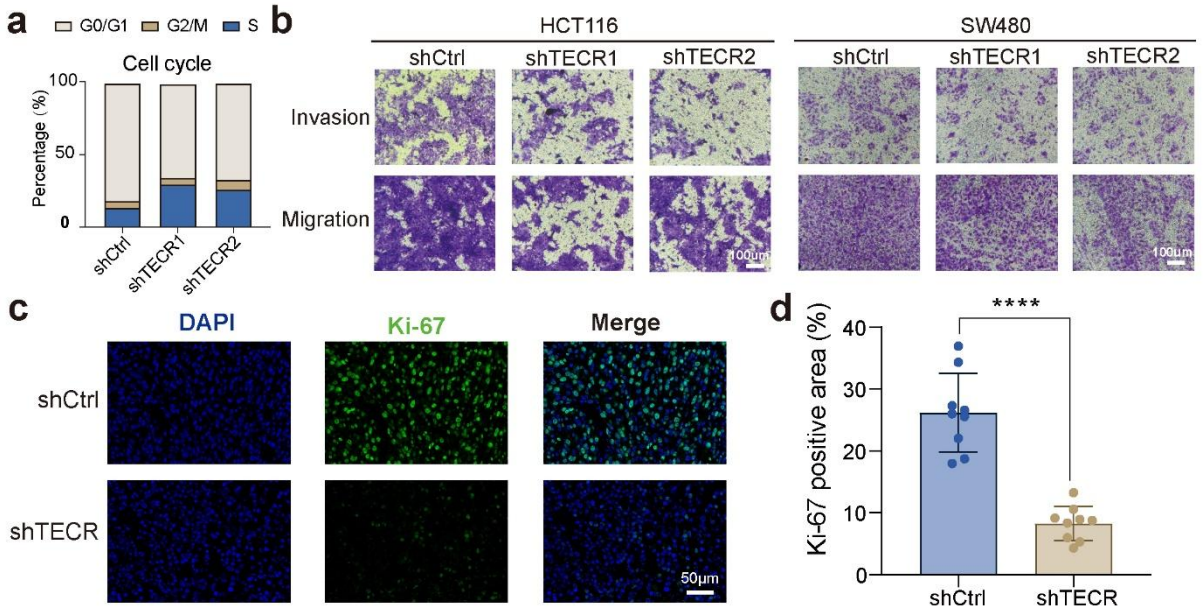

315

316 **Fig. S10 | TECR knockdown suppresses CRC cell proliferation and progression. a,** Cell cycle

317 arrest of TECR-KD HCT116 cells. **b,** TECR-KD suppresses CRC cell invasion and migration. **c,**

318 Representative images of Ki-67 immunofluorescence staining of xenograft tumors. Scales bar, 50 um.

319 **d,** Quantification of Ki-67 staining of (**c**) (n = 9/group). Data are presented as mean ± SD. ****p <

320 0.0001 by Student's t test.

321

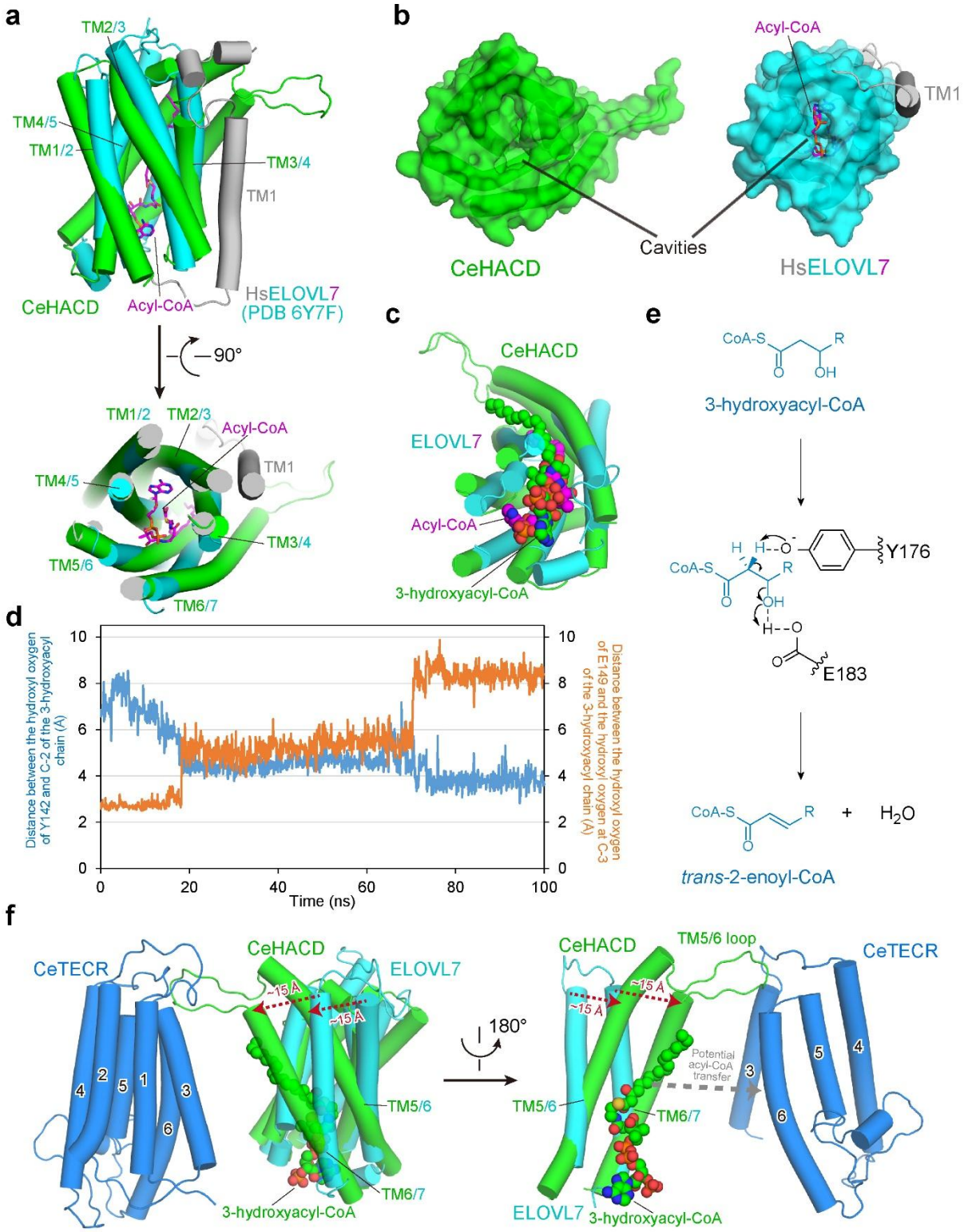

Fig. S11 | **Structural features of HACD. a,** Superimposition of *C. elegans* HACD subunit with human ELOVL7. The acyl-CoA-bound ELOVL7 (PDB 6Y7F) are colored light grey and cyan. The acyl-CoA substrate bound with ELOVL7 is shown in magenta sticks. The *C. elegans* HACD subunit is colored

green. **b,** HACD and ELOVL7 share similar central cavities formed by TM1-6 of HACD and TM2-7 of ELOVL7. **c,** The docked 3-hydroxyacyl-CoA substrate within CeHACD occupies a position roughly similar to that for acyl-CoA substrate in ELOVL7. **d,** The distances between Y142 or E149 in TM5 of CeHACD and the C-2 or C-3 positions of the 3-hydroxyacyl-CoA substrate throughout the 100 ns molecular dynamics (MD) simulation trajectory. Both Y142 and E149 remain in close proximity to the C-2 and C-3 positions of the 3-hydroxyacyl-CoA substrate throughout most of the simulation trajectory (from 18 ns to 70 ns). **e,** Proposed dehydration mechanism of human HACD2. The tyrosine is likely responsible for abstracting a proton from the C-2 position, and the glutamate residue may facilitate the elimination of the hydroxyl group at the C-3 position of 3-hydroxyacyl-CoA substrate. **f,** HACD exhibits an obvious shift and rotation towards TECR compared to ELOVL7. This movement is probably to facilitate transfer of product from HACD to TECR for catalysis coupling. The docked 3-hydroxyacyl-CoA substrate for HACD is shown in spheres.

341 **Table S1 | Cryo-EM data collection, refinement, and validation statistics.**

	C. elegans HACD-TECR (EMD-68536) (PDB 22OF)	Human HACD2-TECR (EMD-38493)
Data collection and processing		
Magnification	105,000	105,000
Voltage (kV)	300	300
Electron exposure (e^{-}/Å^2)	52.76	58.09
Defocus range (μm)	-1.5- -2.0	-1.0- -2.0
Pixel size (Å)	0.85	0.83
Symmetry imposed	C1	C1
Initial particle images (no.)	35,015,130	4,851,341
Final particle images (no.)	131,428	67,876
Map resolution (Å)	3.60	6.32
FSC threshold	0.143	0.143
Map resolution range (Å)	3.0-5.0	
Refinement		
Initial model used (PDB code)	AF2 model	
Model resolution (Å)	3.6/4.0	
FSC threshold	0.143/0.5	
Model composition		
Non-hydrogen atoms	4093	
Protein residues	515	
Ligands	1	
B factors (Å^2)		
Protein	117.45	
Ligand	111.17	
R.m.s. deviations		
Bond lengths (Å)	0.004	
Bond angles (°)	0.729	
Validation		
MolProbity score	1.80	
Clashscore	10.33	
Poor rotamers (%)	0.00	
Ramachandran plot		
Favored (%)	96.09	
Allowed (%)	3.72	
Disallowed (%)	0.20	

342